*Pol. J. Environ. Stud. Vol. XX, No. X (XXXX), 1-11*
DOI: *10.15244/pjoes/204567* ONLINE PUBLICATION DATE:

*Short Communication*

# Spatiotemporal Evolution and Regional Disparities in the Carbon Reduction Potential of Fertilized Straw Utilization in China

**Zheng Liu[1], Yingming Zhao[1], Yuanxin Li[1], Xinyu Liu[1, 2]***

[1]Liaoning Academy of Agricultural Sciences, Shenyang, 110161, China
[2]Organic Cycle Research Institute (Suzhou), China Agricultural University, Suzhou, 215100, China

*Received: 17 March 2025*
*Accepted: 1 May 2025*

## Abstract

The fertilized utilization of straw is a crucial strategy for green agricultural development and carbon reduction in China. However, regional disparities in resource endowment and utilization create a complex spatial carbon emission reduction potential pattern. This study systematically analyzes the total straw and nutrient resources, as well as the spatiotemporal evolution of carbon reduction potential from fertilized straw utilization across 31 provinces from 2014 to 2023. The Theil index quantifies regional imbalances, while Moran's I and local spatial autocorrelation identify clustering patterns. Results indicate that China's total straw resources remained stable, with the highest concentration in the northeastern and central agricultural regions. The carbon reduction potential increased from 18.15 to 20.00 million tons, with nitrogen contributing 85% of the total reduction. The Theil index reveals narrowing regional disparities, though internal imbalances persist in the east. Spatial analysis highlights significant clustering, with the northeast and central regions showing strong "high-high" aggregation, while eastern coastal and western areas exhibit "low-low" clustering. Strengthening regional coordination, optimizing resource allocation, and promoting technology adoption are essential to reducing disparities and enhancing the national carbon reduction potential, contributing to China's green agricultural transformation and "dual carbon" goals.

**Keywords:** straw, resource utilization, carbon emission reduction, Theil index, spatial autocorrelation

## Introduction

Crop straw, the largest agricultural biomass resource globally, has emerged as a pivotal element in agroecological transformation through sustainable management [1]. According to FAO statistics, approximately 2.03 billion tons of crop residues are generated worldwide annually, yet underutilization of 60% results in wasted energy potential equivalent to 470 million tons of standard coal [2, 3]. Despite maintaining grain production exceeding 650 million tons in China for 19 consecutive years, 2023 witnessed 867 million tons of straw production with persistent open-field burning rates of 12-15% [4, 5]. This resource mismanagement creates a dual environmental crisis: annual emissions of 210 million tons of $CO_2$ equivalent and 290,000 tons

*e-mail: liuxinyu@slaas.cn
°ORCID iD: 0000-0001-5655-1301

of $PM_{2.5}$ from burning practices, compounded by excessive fertilizer use contributing 7.3% of national carbon emissions and 51.2% originating from nitrogen fertilizer production [6, 7]. Addressing these challenges necessitates synergistic mechanisms integrating straw valorization with fertilizer substitution.

The carbon mitigation benefits of fertilizer-oriented straw utilization exhibit multi-dimensional synergies [8]. From material cycling perspectives, each ton of straw substitutes 0.15 tons of urea, 0.03 tons of diammonium phosphate, and 0.12 tons of potassium chloride, directly reducing industrial emissions [9, 10]. Soil carbon sequestration analysis reveals 18.7-24.3% increases in topsoil organic carbon stocks through long-term straw incorporation, with sequestration rates reaching 0.35-0.72 t/ha·yr [11]. System optimization further demonstrates a 12.7 kg $CO_2$e/t reduction in indirect emissions from transportation and burning [12]. Despite progress, three scientific barriers persist: (1) Inadequate understanding of spatial heterogeneity, with current studies disproportionately focusing on Northeast China's black soil region and North China Plain [13, 14]; (2) Insufficient temporal resolution, as most analyses rely on cross-sectional data or sub-five-year sequences, failing to capture long-term dynamics under China's dual-carbon strategy; (3) Absence of policy coordination frameworks integrating resource endowment, technological efficiency, and institutional environments.

The study's original contributions are evident in three dimensions. Methodologically, it develops an innovative assessment framework that integrates spatial econometrics with system dynamics, overcoming the scale limitations of conventional life cycle assessment (LCA) methods. Theoretically, it quantifies the spatial spillover effects of straw utilization, advancing locational optimization theory in agroecological engineering. Practically, it proposes a "zoning-tiering-classification" optimization strategy, directly supporting China's Agricultural and Rural Emission Reduction and Carbon Sequestration Implementation Plan.

## Materials and Methods

### Data Sources

This study integrates multi-dimensional authoritative datasets, adhering to open science principles. Crop production data (2015-2024) for staple crops (rice, wheat, maize) and cash crops (cotton, rapeseed) were extracted from the China Statistical Yearbook (National Bureau of Statistics) and cross-validated via the official portal (http://www.stats.gov.cn). Fertilizer application data (N, $P_2O_5$, $K_2O$) were sourced from the China Rural Statistical Yearbook (Ministry of Agriculture and Rural Affairs, 2015-2024 editions) with full temporal coverage. Provincial administrative boundaries (1:4,000,000 scale) were obtained from the National Geomatics Center of China. For East Asia, climate zoning coefficients followed the national standard GB/T 34808-2017. Straw-to-grain ratios were adjusted using FAO's Crop Residue Management Guidelines (2021).

### Straw Nutrient Resource Estimation

Straw yield was calculated based on crop economic output and straw-to-grain ratios. Nutrient availability was determined through stoichiometric relationships between straw yield and elemental composition (Table 1). Calculations focused on macronutrients (N, P, K) using the following Equations [15]:

$$M_{t-dry} = \sum_{i}^{n} (C_i \times R_i \times \lambda_i)$$

$$M_{tN} = M_{t-dry} \times N_i$$

$$M_{tP_2O_5} = M_{t-dry} \times P_i \times 2.29$$

$$M_{tK_2O} = M_{t-dry} \times K_i \times 1.20$$

where $M_{t-dry}$, $M_{tN}$, $M_{tP_2O_5}$, and $M_{tK_2O}$ represent the total straw yield, nitrogen nutrient content, phosphorus nutrient content, and potassium nutrient content, respectively. $N_i$, $P_i$, and $K_i$ denote the dry-matter nutrient content ratios of nitrogen, phosphorus, and potassium in the straw of crop iii. $\lambda_i$ is the climate zoning adjustment coefficient, assigned as follows to enhance regional adaptability: 1.05 for the humid Northeast region, 0.97 for the semi-arid North China region, and 1.12 for the rainy Southern region. The coefficients 2.29 and 1.20 represent the conversion factors for elemental phosphorus to $P_2O_5$ and elemental potassium to $K_2O$, respectively.

Table 1. Ratios of straw to grain and dry matter nutrient content proportions for crops.

| Crop | Straw-to-grain ratio | N/% | P/% | K/% |
|---|---|---|---|---|
| Rice | 1.01 | 0.91 | 0.13 | 1.89 |
| Wheat | 1.37 | 0.65 | 0.08 | 1.05 |
| Maize | 1.10 | 0.92 | 0.15 | 1.18 |
| Soybean | 1.44 | 1.81 | 0.20 | 1.17 |
| Potato | 0.77 | 1.25 | 0.15 | 1.42 |
| Cotton | 3.10 | 1.24 | 0.15 | 1.02 |
| Peanut | 1.26 | 1.82 | 0.16 | 1.09 |
| Rape | 2.71 | 0.87 | 0.14 | 1.94 |
| Sugarcane | 0.10 | 1.10 | 0.14 | 1.10 |

## Carbon Mitigation Potential Estimation of Straw Fertilizer Substitution

This study established a dynamic assessment model integrating regional straw production and nutrient equivalency to quantify the carbon reduction potential of fertilizer-oriented straw utilization in replacing synthetic fertilizers. The methodology calculates emission reductions by comparing baseline fertilizer-induced emissions with post-substitution scenarios through the following Equations:

$$C_{F-S} = C_F - C_S$$

$$C_F = \sum F_{ij} \times q_i$$

$$C_S = \sum C_{ij} \times q_i$$

where $C_{F-S}$ represents the carbon emission reduction potential from straw fertilization, $C_F$ denotes the total carbon emissions from chemical fertilizer application, and $C_S$ represents the carbon emissions reduced by replacing chemical fertilizers with straw nutrients. $F_{ij}$ is the actual amount of fertilizer type iii applied in region *j*, while $C_{ij}$ is the amount of straw-derived nutrients that replace fertilizer type *i* in region *j*. $q_i$ refers to the carbon emission coefficient for fertilizer type *i*. In this study, the carbon emission coefficients for nitrogen (N), phosphorus (P), and potassium (K) fertilizers are set as 2.116 kg $CO_2$e/kg, 0.636 kg $CO_2$e/kg, and 0.180 kg $CO_2$e/kg, respectively.

## Spatiotemporal Evolution of Carbon Mitigation through Straw Fertilization

To quantify regional disparities in agricultural carbon mitigation across China's 31 provinces, we employed the Theil index, an entropy-based statistical measure for assessing resource distribution inequality. This decomposition approach enables the identification of inter-regional and intra-regional disparity sources, providing theoretical foundations for spatial optimization.

### *Theil Index Formulation*

The generalized Theil index is calculated as [16]:

$$T = \frac{1}{N}\sum_{i=1}^{N}\left(\frac{y_i}{\bar{y}}\ln\frac{y_i}{\bar{y}}\right) = T_Q + T_D$$

where *T* represents the total Theil index, reflecting the overall inequality in the distribution of carbon emission reduction potential across provinces. *N* is the total number of provinces, $y_i$ denotes the carbon mitigation value of province *i*, and $\bar{y}$ represents the national mean carbon mitigation value. A higher Theil index indicates greater regional disparity in carbon reduction potential.

### *Inter-Regional Disparity ($T_Q$)*

$$T_Q = \sum_{r=1}^{R}\frac{N_r}{N}\frac{\bar{y_r}}{\bar{y}}\ln\frac{\bar{y_r}}{\bar{y}}$$

where *R* represents the number of regions, $N_r$ is the number of provinces in region *r*, and $\bar{y_r}$ denotes the mean mitigation value of region *r*.

### *Intra-Regional Disparity ($T_D$)*

$$T_D = \sum_{r=1}^{R}\frac{N_r}{N}T_r$$

where $T_r$ represents the Theil index for region *r*.

## Spatial Distribution Patterns and Regional Clustering Characteristics of Carbon Mitigation

This study employs spatial autocorrelation analysis encompassing global and local perspectives to investigate the spatial distribution patterns and regional clustering characteristics of carbon mitigation potential through straw fertilization [17, 18]. This geostatistical approach quantitatively evaluates spatial dependence among adjacent regions, revealing spatial aggregation patterns and regional disparities in agricultural carbon management.

### *Global Spatial Autocorrelation*

The global Moran's Index (Moran's I) was calculated to assess the overall spatial distribution patterns across China:

$$I = \frac{n\sum_{i=1}^{n}\sum_{j=1}^{n}W_{ij}(x_i-\bar{x})(x_j-\bar{x})}{\sum_{i=1}^{n}\sum_{j=1}^{n}W_{ij}\sum_{i=1}^{n}(x_i-\bar{x})^2}$$

where *n* represents the number of provincial units (31), $W_{ij}$ is the spatial weight matrix indicating the adjacency relationship between unit *i* and *j*. $x_i$ and $x_j$ denote the carbon mitigation values of provinces *i* and *j*, respectively, and $\bar{x}$ is the national mean carbon mitigation value. The value of Moran's I ranges between [−1,1]. I>0 indicates a positive spatial correlation, meaning that similar values tend to cluster (i.e., high-carbon reduction areas or low-carbon reduction areas group together). I<0 suggests a negative spatial correlation, implying that dissimilar values are spatially adjacent (i.e., high-carbon reduction areas are surrounded by low-carbon reduction

areas and vice versa). I = 0 represents a random spatial distribution with no discernible clustering pattern.

*Local Spatial Autocorrelation (LISA)*

Local Indicators of Spatial Association (LISA) were computed to identify localized clustering patterns:

$$I_i = \frac{n(x_i - \bar{x}) \sum_{j=1}^{n} W_{ij}(x_j - \bar{x})}{\sum_{i=1}^{n}(x_i - \bar{x})^2}$$

where $I_i$ represents the local spatial autocorrelation index for province *i*. $I_i$>0 indicates a positive spatial correlation, which includes "high-high" clustering and "low-low" clustering. $I_i$<0 suggests a negative spatial correlation, which includes "high-low" clustering and "low-high" clustering, reflecting significant spatial disparities in carbon mitigation between neighboring regions.

## Division of the Study Area

In accordance with the classification standards outlined in the China Regional Economic Statistical Yearbook and the policy adjustments specified in the State Council's Guiding Opinions on Promoting Coordinated Regional Development ([2018] No. 24), this study divides mainland China's 31 provincial-level administrative divisions (excluding Hong Kong, Macao, and Taiwan) into three major economic regions:

Eastern Region: Liaoning, Hebei, Beijing, Tianjin, Shandong, Jiangsu, Shanghai, Zhejiang, Fujian, Guangdong, and Hainan.

Central Region: Heilongjiang, Jilin, Shanxi, Henan, Anhui, Hubei, Hunan, and Jiangxi.

Western Region: Sichuan, Chongqing, Guizhou, Yunnan, Tibet Autonomous Region, Shaanxi, Gansu, Qinghai, Ningxia Hui Autonomous Region, Xinjiang Uygur Autonomous Region, Inner Mongolia Autonomous Region, and Guangxi Zhuang Autonomous Region.

# Results

## Straw Yield of 31 Provinces in China

From 2014 to 2023, China's crop residue production exhibited distinct spatiotemporal distribution patterns across provincial-level administrative regions (Fig. 1). Geospatial analysis revealed pronounced regional disparities, with agricultural powerhouses in northern China, including Heilongjiang, Henan, and Shandong, maintaining consistently high output levels. Notably, Heilongjiang and Henan emerged as national leaders in residue generation, both sustaining annual production exceeding $8.0\times10^8$ t throughout the study period. In contrast, eastern coastal regions such as Shanghai and Hainan demonstrated substantially lower outputs, with annual averages below $5.0\times10^6$ t. This spatial heterogeneity strongly correlates with regional

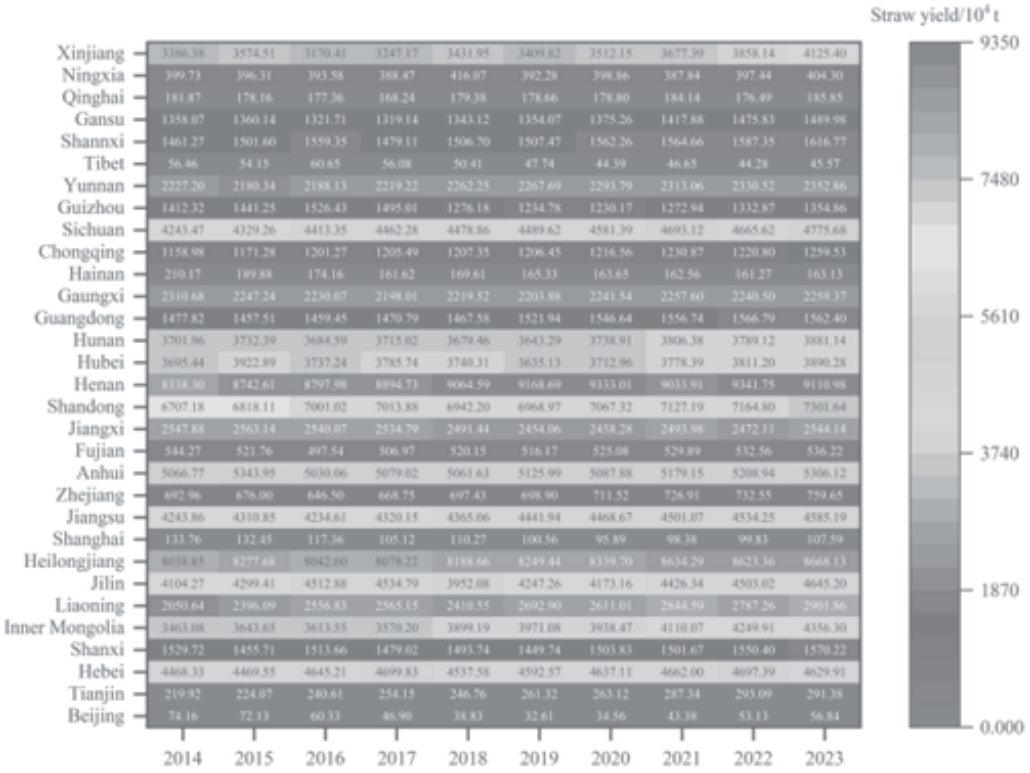


Fig. 1. Straw yield of 31 provinces in China (2014-2023).

variations in cultivated land resources and agricultural activity intensity.

Temporal analysis revealed oscillatory patterns in national residue production over the decade. Several major agricultural provinces displayed moderate growth trends, exemplified by Heilongjiang's residue output increasing from $8.04\times10^8$ t in 2014 to $8.67\times10^8$ t in 2023, representing an average annual growth rate of approximately 1%. Henan Province maintained production dominance despite temporary fluctuations, achieving $9.11\times10^8$ t in 2023. Conversely, Beijing experienced a notable 23.4% reduction in residue generation, declining from $7.42\times10^6$ t to $5.68\times10^6$ t, attributable to urban expansion and arable land conversion. The most striking growth occurred in Xinjiang, where residue production surged by 21.8%, from $3.39\times10^8$ t to $4.13\times10^8$ t, reflecting substantial agricultural expansion in northwest China.

Regional production characteristics are further manifested in crop-specific patterns. Eastern provinces, including Jiangsu and Shandong, maintained stable high outputs of $4.59\times10^8$ t and $7.30\times10^8$ t, respectively, in 2023, primarily from wheat-rice rotation systems. Central agricultural zones encompassing Anhui, Henan, and Hubei demonstrated production stability with marginal increases, exemplified by Anhui's 4.7% growth from $5.07\times10^8$ t to $5.31\times10^8$ t. Western regions displayed the most dynamic changes, particularly Xinjiang's remarkable annual growth rate of 2.2%, which is closely associated with agricultural restructuring and cultivation area expansion in China's western development initiatives.

## Nutrients in China's Straw

China's total crop residue nutrient resources demonstrated a sustained growth trajectory from 2014 to 2023, comprising nitrogen (N), phosphorus (P), and potassium (K) as the primary components (Table 2). Over the decade, the aggregate nutrient content increased from $1.93\times10^7$ t to $2.11\times10^7$ t, representing a 9.05% cumulative growth. Component analysis revealed differentiated growth patterns: nitrogen content rose from $7.34\times10^6$ t to $8.11\times10^6$ t (10.51% increase), phosphorus from $1.04\times10^6$ t to $1.14\times10^6$ t (10.32%), and potassium from $1.09\times10^7$ t to $1.18\times10^7$ t (7.96%). The proportional distribution remained stable throughout the study period, with potassium dominating at 56-58% of total nutrients, followed by nitrogen (37-39%), while phosphorus constituted approximately 5%.

Post-2019 acceleration marked the nutrient growth patterns, particularly in nitrogen resources, which expanded from $7.66\times10^6$ t to $8.11\times10^6$ t at an annualized rate of 1.44%. Despite moderate relative growth, potassium maintained its quantitative dominance, with absolute quantities increasing by $8.70\times10^6$ t over the decade. Stability analysis through coefficient of variation (CV) measurements revealed potassium's superior interannual consistency (CV = 2.36%), compared to phosphorus (3.01%) and nitrogen (3.12%). This low variability profile confirms the overall stability of China's crop residue nutrient resources, with potassium demonstrating particularly robust supply reliability across agricultural production systems.

Table 2. Total Nitrogen, Phosphorus, and Potassium Nutrients in China's straw.

| Year | Total N nutrients/$10^4$ t | Total P nutrients/$10^4$ t | Total K nutrients/$10^4$ t | Total nutrients/$10^4$ t |
|---|---|---|---|---|
| 2014 | 733.5430 | 103.5607 | 1093.3910 | 1930.495 |
| 2015 | 750.6480 | 106.3363 | 1120.1650 | 1977.149 |
| 2016 | 749.0228 | 105.9216 | 1114.0760 | 1969.0200 |
| 2017 | 755.8312 | 106.4919 | 1119.6020 | 1981.9250 |
| 2018 | 756.3135 | 106.4162 | 1116.3210 | 1979.0510 |
| 2019 | 765.4831 | 107.5803 | 1123.8490 | 1996.9130 |
| 2020 | 775.4391 | 108.7992 | 1136.2460 | 2020.4840 |
| 2021 | 784.3546 | 110.5336 | 1155.8070 | 2050.6950 |
| 2022 | 797.7446 | 112.2340 | 1165.1930 | 2075.1720 |
| 2023 | 810.6476 | 114.2475 | 1180.3720 | 2105.2680 |
| Total | 7679.0277 | 1082.1214 | 11325.0231 | 20086.1722 |
| Average | 767.9028 | 108.2121 | 1132.502 | 2008.617 |
| Growth rate | 10.51% | 10.32% | 7.96% | 9.05% |
| Variation coefficient | 3.120% | 3.007% | 2.362% | 2.679% |

## Carbon Emission Reduction Potential of Fertilized Straw Utilization in China

China's decarbonization potential through straw fertilizer utilization demonstrated consistent growth from 2014 to 2023, with total carbon reduction capacity increasing from $1.81\times10^7$ t to $2.00\times10^7$ t, representing a 10.23% cumulative enhancement (Fig. 2). Element-specific analysis revealed differentiated contribution patterns: nitrogen-based reduction dominated the process, expanding from $1.55\times10^7$ t to $1.72\times10^7$ t (10.50% growth) while maintaining a >85% share of total reductions. Phosphorus contributions grew 10.33%, from $6.59\times10^5$ t to $7.27\times10^5$ t, providing stable baseline support despite its modest 3-4% proportion. Potassium exhibited complementary functionality with a 7.96% increase ($1.97\times10^6$ t to $2.12\times10^6$ t), consistently accounting for approximately 10% of total mitigation capacity.

Post-2019 acceleration marked a pivotal transition, with the annual nitrogen reduction growth rate doubling to 1.44% during 2019-2023. This phase coincided with agricultural expansion, widespread adoption of resource recovery technologies, and enhanced policy incentives. Concurrent stabilization occurred in phosphorus (1.8% annual growth) and potassium (1.6%) contributions, reinforcing integrated straw utilization's decarbonization efficacy. Structural analysis confirmed remarkable stability in elemental contribution ratios throughout the decade: nitrogen maintained an 85±0.5% share, potassium 10±0.3%, and phosphorus 3.5±0.2%. This persistent proportionality demonstrates effective synergy among nutrient-specific reduction mechanisms, ensuring comprehensive realization of carbon mitigation potential through optimized elemental coordination.

## Regional Variations in the Carbon Reduction Potential of Straw Fertilization

Between 2014 and 2023, the Theil index measuring the carbon reduction potential of straw fertilizer utilization in China showed minor fluctuations, stabilizing within the range of 3.84 to 3.90 (Table 3). This pattern suggests that regional disparities in carbon mitigation benefits persisted but did not widen significantly. The national Theil index decreased slightly from 3.87 in 2014 to 3.84 in 2023, indicating a gradual spatial equalization of carbon reduction efficiency across the country.

Geographically, eastern China consistently exhibited the highest Theil index, reaching 1.86 in 2023, primarily due to its industrialized economy, complex agricultural systems, and uneven provincial adoption of straw utilization technologies. These factors amplified intra-regional differences in carbon mitigation outcomes. In contrast, central China demonstrated remarkable stability, with its Theil index hovering between 0.54 and 0.57 over the decade, reflecting balanced and coordinated practices in straw fertilization. Western China emerged as the most improved region, with its Theil index declining significantly from 1.48 in 2014 to 1.41 in 2023. This progress aligns with targeted green agricultural policies promoting straw return and composting, which have enhanced regional coordination in carbon reduction.

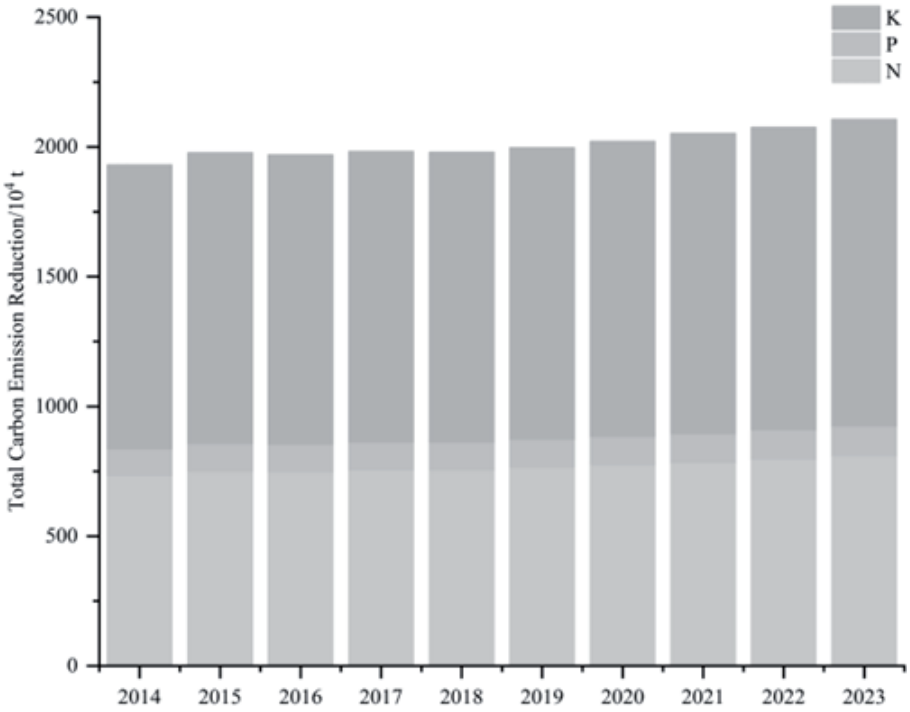


Fig. 2. Carbon Emission reduction potential of fertilized straw utilization in China (2014-2023).

Notably, intra-regional Theil indices remained extremely low (around 0.01) across all zones, implying minimal internal disparities within the eastern, central, and western regions. The dominant contributor to national inequality stemmed from inter-regional differences, driven by variations in agricultural resources, policy implementation intensity, and economic development levels.

Temporal trends revealed divergent pathways. Eastern China experienced a marginal rise in its Theil index, signaling persistent utilization gaps among its provinces. Conversely, western China achieved substantial harmonization through large-scale straw recycling initiatives, particularly after 2018, when the national Theil index stabilized near 3.85. This stabilization marks the synergistic effects of policy interventions and technological dissemination, such as the widespread adoption of straw incorporation techniques to reduce chemical fertilizer use.

The evolving spatial patterns underscore the critical influence of region-specific agricultural modernization strategies. While the western regions benefit from centralized policy-driven transformations, the eastern areas face challenges reconciling industrial development with sustainable farming practices. These dynamics highlight the need for differentiated governance approaches to optimize nationwide straw-derived carbon mitigation benefits.

## Global Spatial Autocorrelation Analysis

The global spatial autocorrelation analysis of carbon mitigation potential through straw fertilizer utilization revealed consistent positive associations from 2014 to 2023, as evidenced by Moran's I indices ranging between 0.211 and 0.243 (Table 4). These statistically significant values ($p$<0.05 throughout the study period) confirm non-random spatial clustering patterns, with provinces exhibiting either high-value or low-value agglomerations in decarbonization capacity. The strongest spatial autocorrelation emerged in 2016 (Moran's I = 0.243, z-score = 2.331), potentially associated with nationwide agricultural policy intensification and concentrated promotion of straw utilization technologies during this pivotal year.

Interannual analysis demonstrated remarkable stability in spatial clustering characteristics, with Moran's I maintaining values above 0.210 despite minor fluctuations. Standard deviation parameters remained constrained between 0.113 and 0.124, confirming measurement reliability. While 2018 and 2020 showed marginally lower indices (0.211), these transient variations likely reflect short-term fluctuations in cultivation areas and utilization efficiencies rather than structural spatial pattern alterations.

Geospatial distribution patterns revealed distinct clustering mechanisms. High-capacity provinces are predominantly concentrated in northeastern and central China's grain production belts, benefiting from abundant straw resources and policy advantages. Conversely, western and selected eastern regions formed persistent low-capacity clusters, constrained by resource limitations and suboptimal utilization rates. The sustained spatial autocorrelation underscores the enduring influence of regional agricultural infrastructure development and technology diffusion patterns on decarbonization potential realization.

## Local Spatial Autocorrelation Analysis

Local spatial autocorrelation analysis delineated evolving provincial patterns in straw fertilizer-based carbon mitigation potential across distinct clustering types: high-high (HH), low-low (LL), high-low (HL), and low-high (LH). Longitudinal examination of 2014, 2019, and 2023 data revealed stabilized spatial configurations with intensified HH concentration and persistent LL dispersion (Fig. 3). Central and northeastern provinces (Henan, Heilongjiang, Jilin) demonstrated strong regional coordination, contrasting

Table 3. Theil index of carbon emission reduction potential from fertilized straw utilization in China (2014-2023).

| Year | Eastern region | Central region | Western region | Intraband | Total |
|---|---|---|---|---|---|
| 2014 | 1.83 | 0.55 | 1.48 | 0.01 | 3.87 |
| 2015 | 1.86 | 0.54 | 1.50 | 0.01 | 3.90 |
| 2016 | 1.80 | 0.55 | 1.51 | 0.01 | 3.87 |
| 2017 | 1.80 | 0.54 | 1.52 | 0.01 | 3.88 |
| 2018 | 1.84 | 0.56 | 1.45 | 0.01 | 3.86 |
| 2019 | 1.80 | 0.56 | 1.47 | 0.01 | 3.85 |
| 2020 | 1.82 | 0.56 | 1.47 | 0.01 | 3.86 |
| 2021 | 1.81 | 0.56 | 1.45 | 0.01 | 3.83 |
| 2022 | 1.85 | 0.56 | 1.43 | 0.01 | 3.85 |
| 2023 | 1.86 | 0.57 | 1.41 | 0.01 | 3.84 |

Table 4. Global Moran's I index of carbon emission reduction potential from fertilized straw utilization (2014-2023).

| Year | Moran's I | Standard deviation | z | p |
|---|---|---|---|---|
| 2014 | 0.218 | 0.116 | 2.119 | 0.017 |
| 2015 | 0.228 | 0.118 | 2.206 | 0.014 |
| 2016 | 0.243 | 0.124 | 2.331 | 0.01 |
| 2017 | 0.236 | 0.116 | 2.273 | 0.012 |
| 2018 | 0.211 | 0.12 | 2.066 | 0.019 |
| 2019 | 0.223 | 0.114 | 2.159 | 0.015 |
| 2020 | 0.211 | 0.115 | 2.065 | 0.019 |
| 2021 | 0.217 | 0.113 | 2.116 | 0.017 |
| 2022 | 0.218 | 0.115 | 2.118 | 0.017 |
| 2023 | 0.219 | 0.119 | 2.133 | 0.016 |

with fragmented spatial associations in eastern coastal areas (Beijing, Zhejiang) and western regions (Qinghai, Ningxia).

Persistent HH clusters emerged across agricultural heartlands, including Hebei, Jilin, Heilongjiang, Jiangsu, Anhui, Shandong, Henan, and Hubei, maintaining stable spatial autocorrelation throughout the study period. These regions exhibited 1.5-2.3×$10^7$ t annual carbon mitigation capacity, supported by intensive crop cultivation (7.8-9.1×$10^7$ t straw production) and advanced resource recovery rates (68-72%). Northeastern provinces exemplified this pattern, where Heilongjiang's mitigation potential increased from 1.98×$10^7$ t to 2.31×$10^7$ t, correlating with a 12.5% improvement in straw utilization efficiency.

LL clusters are concentrated in economically developed but agriculturally limited regions (Beijing, Tianjin, Shanghai, Zhejiang, Fujian, Guangdong), demonstrating consistently low mitigation capacities below 5.0×$10^5$ t. These areas showed 38-45% lower straw recovery rates than national averages, with Beijing's mitigation potential declining from 6.84×$10^4$ t to 5.12×$10^4$ t despite 15% urban agricultural expansion.

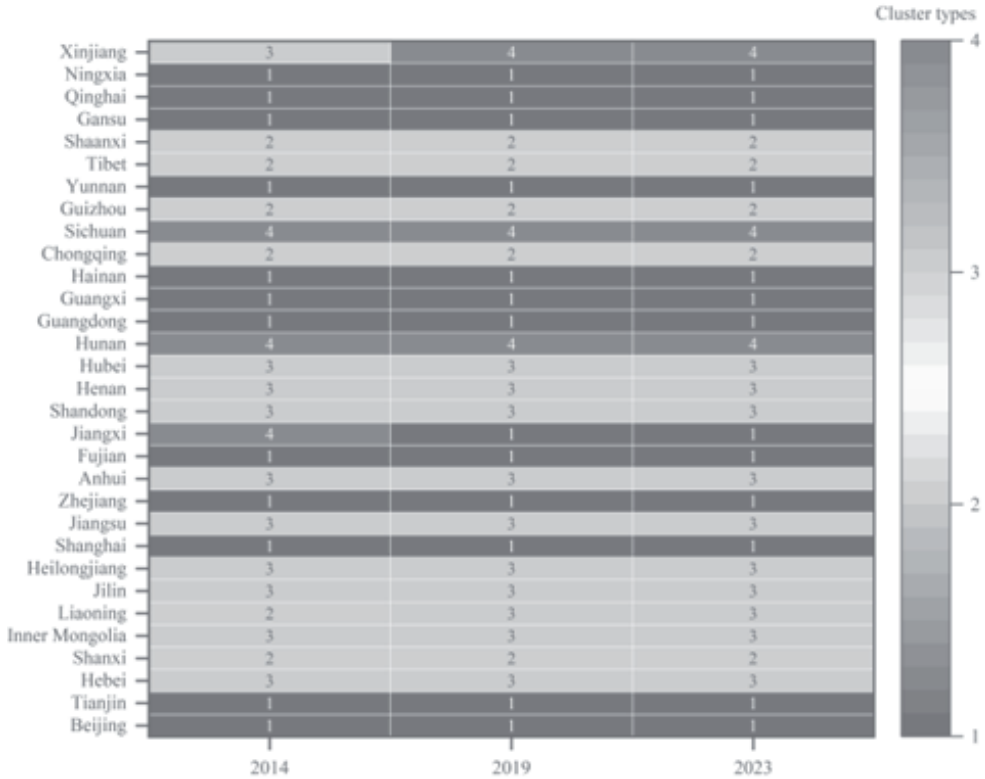


Fig. 3. Cluster types of carbon emission reduction potential from fertilized straw utilization in 2014, 2019, and 2023.

Spatiotemporal transitions revealed dynamic provincial trajectories. Liaoning transitioned from the LH (2014) to the HH cluster (2023), achieving $1.42\times10^7$ t mitigation capacity through enhanced green agricultural policies and a 25% improvement in the straw recovery rate. Conversely, Jiangxi shifted from the HL to the LL cluster, reflecting an 18% reduction in mitigation potential ($2.07\times10^6$ t to $1.71\times10^6$ t) associated with technology diffusion lags. Western regions displayed persistent spatial disparities, with Xinjiang maintaining HL status ($3.85\times10^6$ t mitigation capacity) despite 32% higher provincial utilization rates than neighboring areas.

This spatial evolution underscores the dual influence of endogenous agricultural capacity and exogenous policy interventions. HH cluster stability correlates with regional straw production exceeding $6.5\times10^7$ t and policy investment intensity above 120 CNY/t, while LL regions demonstrate inverse relationships between economic development levels (per capita GDP>12,000 USD) and agricultural decarbonization priorities.

## Discussion

As the most abundant biomass waste generated during agricultural production, the resource utilization of crop straw has long been a pivotal research topic in agricultural science [19, 20]. Current studies predominantly focus on fertilizer-oriented utilization strategies, including straw return to fields, mulching, biochar production, and organic fertilizer preparation – all representing organic recycling approaches that reintegrate straw into agricultural ecosystems and soil nutrient cycles [21, 22]. Notably, this circular process demonstrates significant carbon sequestration and emission reduction effects, a phenomenon consistently validated by multiple studies [23]. Given China's status as a major agricultural producer generating massive quantities of straw annually, assessing the carbon mitigation potential of straw-based fertilization necessitates preliminary quantification of national straw resources.

Considerable discrepancies exist among existing straw resource estimates, primarily attributable to variations in crop selection and straw-to-grain ratios. Yang et al. estimated 772 million tons (Mt) of straw production in 2020 using region-specific ratios for 13 crops [24], while Liu et al. reported approximately 800 Mt based on uniform ratios for 15 crops [25]. Aligning with Xu et al., this study employs standardized straw-to-grain ratios for 9 major crops, considering collection feasibility, yielding annual straw outputs of 830 Mt (2020), 846 Mt (2021), 855 Mt (2022), and 867 Mt (2023) [26].

Regarding straw nutrient quantification, existing research predominantly concentrates on regional analyses (Northeast China, Yellow River Basin, Yangtze River Delta) or specific crops (wheat, maize, rice), with national-scale nutrient estimates largely outdated pre-2020 [27]. Our findings reveal 21.1 Mt of total nutrient content in 2023 straw resources, with potassium constituting 56.07% (11.83 Mt). Comparative analysis with China's 2023 fertilizer application data (26.2 Mt of pure nutrients excluding compound fertilizers: 16.0 Mt nitrogen, 5.4 Mt phosphorus, and 4.8 Mt potassium) indicates that straw nutrients could potentially substitute 50.63% of nitrogen, 20.37% of phosphorus, and 245.83% of potassium fertilizer demand.

The carbon mitigation potential of straw fertilization was evaluated through life-cycle emission factors adapted to China's fertilizer production context. Results demonstrate increasing carbon reduction capacity, reaching 20.0 Mt $CO_2$-eq in 2023, equivalent to 52.4% of total fertilizer manufacturing emissions (38.2 Mt $CO_2$-eq). Regional analysis reveals complete offset potential for specific nutrient emissions in major agricultural provinces (e.g., Jilin and Heilongjiang). Spatial patterns show higher mitigation effects in nitrogen-intensive grain belts and enhanced ecological benefits in phosphorus/potassium-rich regions.

Theil index analysis indicates decreasing regional disparities in mitigation potential, particularly in western China, reflecting improved straw utilization under green agriculture policies. However, persistent imbalances in eastern regions suggest economic and agricultural structural influences. Spatial autocorrelation reveals significant clustering patterns: "high-high" agglomerations in Northeast/Central China versus "low-low" clusters in coastal and western areas. Dynamic shifts, such as Liaoning's transition from "low-high" to "high-high" status, highlight policy effectiveness, while Jiangxi's regression to "low-low" signals efficiency decline risks. Future strategies should emphasize inter-regional collaboration, technology transfer, and policy coordination to optimize spatial patterns and narrow regional mitigation gaps.

## Conclusions

This study systematically evaluates the spatiotemporal evolution of China's straw resources, nutrient content, and carbon mitigation potential through straw fertilization from 2014 to 2023. Key findings reveal sustained growth in both straw availability and associated carbon reduction capacity, accompanied by pronounced regional disparities and distinct spatial clustering patterns. The primary agricultural zones in Northeast and Central China maintain superior performance, exhibiting stable "high-high" clustering characteristics in carbon mitigation potential. Conversely, coastal eastern regions and partial western areas demonstrate constrained potential due to resource limitations, forming persistent "low-low" clusters. Theil index analysis indicates mitigated inter-regional disparities at the national scale, while intra-regional imbalances remain significant.

Enhancing straw fertilization efficiency proves crucial for advancing agricultural green transformation and supporting national carbon neutrality objectives. Future strategies should prioritize inter-regional collaboration, resource optimization, and targeted technological breakthroughs in low-performance zones. Implementing these measures will enable balanced improvement of straw valorization benefits nationwide, ultimately providing robust support for carbon reduction and ecological sustainability in the agricultural sector.

## Acknowledgments

This study was supported by the Liaoning Social Science Planning Fund Project (L21CJY016).

## Conflict of Interest

The authors declare no conflict of interest.

## References

1. GUO Z., LIU Y., MENG X., YANG X., MA C., CHAI H., LI H., DING R., NAZAROV K., ZHANG X., HAN Q. The long-term nitrogen fertilizer management strategy based on straw return can improve the productivity of wheat-maize rotation system and reduce carbon emissions by increasing soil carbon and nitrogen sequestration. Field Crops Research. **317**, 109561, **2024**.
2. QIAN B., SHAO C., YANG F. Spatial suitability evaluation of the conversion and utilization of crop straw resources in China. Environmental Impact Assessment Review. **105**, 107438, **2024**.
3. ZHANG J., GE X., QIU X., LIU L., MULDER J., DUAN L. Estimation of carbon sequestration potential and air quality impacts of biochar production from straw in China. Environmental Pollution. **363**, 125304, **2024**.
4. LIANG J., PAN S., XIA N., CHEN W., LI M. Threshold response of the agricultural modernization to the open crop straw burning $CO_2$ emission in China‘s nine major agricultural zones. Agriculture, Ecosystems & Environment. **368**, 109005, **2024**.
5. LIU X., LIU J., LIU Z. Developing a model of propagating the straw burning prohibition policy in Chinese rural communities and exploring its countermeasures. Energy Reports. **11**, 2556, **2024**.
6. XU X., YE Y., LI J., XU Z., SUN M., LI C., ZHANG L., XUE Y. GHG emissions of straw treatments in rural China and scenario simulation based on life cycle perspective. Journal of Cleaner Production. **377**, 134377, **2022**.
7. LIU X., TU S., LIU J., LIU Z. Emission forecasting from open burning of crop straw and policy analysis: The case for China. Energy Reports. **9**, 5659, **2023**.
8. ZHANG L., JIANG G., XIAO R., HOU K., LIU X., LIU X., YUAN P., TIAN F., YIN L., ZHU H., TIAN C., YANG L., YAN X., RONG X., HAN Y. An appropriate amount of straw replaced chemical fertilizers returning reduced net greenhouse gas emissions and improved net ecological economic benefits. Journal of Cleaner Production. **434**, 140236, **2024**.
9. ZHANG Y., YUAN S., GAO W., LUAN H., TANG J., LI R., LI M., ZHANG Q., WANG Y., HUANG S. Long-term manure and/or straw substitution mediates phosphorus species and the phosphorus-solubilizing microorganism community in soil aggregation. Agriculture, Ecosystems & Environment. **378**, 109323, **2025**.
10. WANG Y., LIANG B.-Q., BAO H., CHEN Q., CAO Y.-L., HE Y.-Q., LI L.-Z. Potential of crop straw incorporation for replacing chemical fertilizer and reducing nutrient loss in Sichuan Province, China. Environmental Pollution. **320**, 121034, **2023**.
11. LIU C., SI B., ZHAO Y., WU Z., LU X., CHEN X., HAN X., ZHU Y., ZOU W. Drivers of soil quality and maize yield under long-term tillage and straw incorporation in Mollisols. Soil and Tillage Research. **246**, 106360, **2025**.
12. WANG S., YIN C., LI F., RICHEL A. Innovative incentives can sustainably enhance the achievement of straw burning control in China. Science of The Total Environment. **857**, 159498, **2023**.
13. FANG Y., XU K., GUO X., HONG Y. Identifying determinants of straw open field burning in northeast China: Toward greening agriculture base in newly industrializing countries. Journal of Rural Studies. **74**, 111, **2020**.
14. SONG Y., GAO M., LI Z. Impacts of straw return methods on crop yield, soil organic matter, and salinity in saline-alkali land in North China. Field Crops Research. **322**, 109752, **2025**.
15. SHAO M. Straw Biochar Production and Carbon Emission Reduction Potential in the Yangtze River Economic Belt Region. Polish Journal of Environmental Studies. **34** (3), 2349, **2025**.
16. XU C., WANG B., CHEN J., SHEN Z., SONG M., AN J. Carbon inequality in China: Novel drivers and policy driven scenario analysis. Energy Policy. **170**, 113259, **2022**.
17. CHEN Y., YANG Y., FANG L., ZHAO H., YANG Z., CHEN L., YU H. Spatial effects of the agricultural ecosystem services based on environmental kuznets curve in Mengyin county, China. Heliyon. **9** (5), e15918, **2023**.
18. WU H., ZHENG X., ZHOU L., MENG Y. Spatial autocorrelation and driving factors of carbon emission density of crop production in China. Environmental Science and Pollution Research. **31** (18), 27172, **2024**.
19. WU H., WANG C., MAO H., WEN Y., ZHENG C., ZHANG W., YI S. Value-added bio-products extracted from straw utilized as carriers for pesticide delivery: Innovative repurposing of agricultural waste. Industrial Crops and Products. **223**, 120294, **2025**.
20. NAZAR M., TIAN J., WANG X., WANG S., KHAN N. A., CHENG Y., ZHANG W., XU N., LIU B., DING C. Biological delignification and anaerobic fermentation of wheat straw: A promising approach for sustainable utilization of crop straw bioresources. Industrial Crops and Products. **227**, 120839, **2025**.
21. CHANG F., YUE S., LI S., WANG H., CHEN Y., YANG W., WU B., SUN H., WANG S., YIN L., DENG X. Periodic straw-derived biochar improves crop yield, sequesters carbon, and mitigates emissions. European Journal of Agronomy. **164**, 127516, **2025**.
22. DUAN Z., KANG Z., KONG X., QIU G., WANG Q., WANG T., HAN X., ZHU G., WEN L., XU X., SU Y., YU H. Development of a novel low-temperature-tolerant microbial consortium for efficient degradation and recycling of farmland straw. Journal of Environmental Chemical Engineering. **13** (2), 115884, **2025**.

23. WEI L.E., SONG K., QI Y., SUN S., NI G., ZHOU C., YIN X. Effects of straw returning after anaerobic microbial pretreatment on soil carbon sequestration and emission reduction. Environmental Technology & Innovation. **38**, 104124, **2025**.
24. YANG C.W., XING F., ZHUU J.C., LI R.H., ZHANG Z.Q. Temporal and Spatial Distribution, Utilization Status, and Carbon Emission Reduction Potential of Straw Resources in China. Environmental Science. **44** (2), 1149, **2023**.
25. LIU J.J., YAN X.B., ZHANG M.Y., LIU T.S., SU Z.M. Analysis of yield distribution and utilization of crop straw resources in China. Journal of Agricultural Resources and Environment. **42** (3), 751, **2025**.
26. XU S.Q., CHEN W.J., XIE L.Q., CAI S.Y., JIA K.X., WEI Y.Q. Organic waste resources and nutrient utilization potential in China. Journal of Plant Nutrition and Fertilizers. **28** (08), 1341, **2022**.
27. LIN B.-J., CHENG J., DUAN H.-X., LIU W.-X., DANG Y. P., ZHAO X., ZHANG H.-L. Optimizing straw and nitrogen fertilizer resources for low-carbon sustainable agriculture. Resources, Conservation and Recycling. **209**, 107743, **2024**.